

## CALET on the ISS: The first 5 years

Pier Simone Marrocchesi\* for the CALET Collaboration†

*Dept. of Physical Sciences, Earth and Environment, Via Roma 56, I-53100 Siena, Italy  
and INFN Sezione di Pisa, Largo Bruno Pontecorvo 3, I-56127 Pisa, Italy*

\*E-mail: piersimone.marrocchesi@pi.infn.it

**Abstract**—The CALorimetric Electron Telescope CALET is collecting science data on the International Space Station since October 2015 with excellent and continuous performance. Energy is measured with a deep homogeneous calorimeter (1.2 nuclear interaction lengths, 27 radiation lengths) preceded by an imaging pre-shower (3 radiation lengths, 1mm granularity) providing tracking and  $10^{-5}$  electron/proton discrimination. Two independent sub-systems identify the charge  $Z$  of the incident particle from proton to iron and above ( $Z < 40$ ). CALET measures the cosmic-ray electron+positron flux up to 20 TeV, gamma rays up to 10 TeV, and nuclei up to 1 PeV. In this paper, we report the on-orbit performance of the instrument and summarize the main results obtained during the first 5 years of operation, including the electron+positron energy spectrum and the individual spectra of protons, heavier nuclei and iron. Solar modulation and gamma-ray observations are also concisely reported, as well as transient phenomena and the search for gravitational wave counterparts.

**Keywords:** Cosmic rays; high energy astrophysics; space-borne experiments.

### 1. INTRODUCTION

CALET is a cosmic-ray experiment designed for long-term observations of charged and neutral cosmic radiation on the ISS. The instrument is managed by an international collaboration led by the Japanese Space Agency (JAXA) with the participation of the Italian Space Agency (ASI) and NASA. It was launched on August 19, 2015 with the Japanese carrier H-IIIB, delivered to the ISS by the HTV-5 Transfer Vehicle, and installed on the Japanese Experiment Module Exposure Facility (JEM-EF). The science program of CALET addresses several outstanding questions of high-energy astroparticle physics including the origin of cosmic rays (CR), the possible presence of nearby astrophysical CR sources, the acceleration and propagation of primary and secondary elements in the galaxy, and the nature of dark matter. The design of CALET is optimised for high precision measurements of the electron+positron spectrum with an accurate scan of the energy interval already covered by previous experiments and its extension to the region above 1 TeV. Given the high energy resolution of CALET for electrons, a detailed study of the spectral shape might reveal the presence of nearby sources of acceleration as well as possible indirect signatures of dark matter.<sup>1,2</sup>

With its individual element resolution in the charge identification of cosmic rays, CALET is also carrying out direct measurements of the spectra and relative

†See the last page for the full authors list.

abundances of light and heavy cosmic nuclei<sup>3,4</sup> from proton to iron, in the energy interval from  $\sim 50$  GeV ( $10$  GeV/ $n$ ) for the lighter (heavier) nuclei to several hundred TeV. The abundances of the rare CR trans-iron elements up to  $Z \sim 40$  are studied with a dedicated program of long term observations.<sup>5</sup>

## 2. THE CALET INSTRUMENT

The CALET main telescope is an all-calorimetric instrument comprised of three sub-detectors. The CHarge Detector (CHD) is positioned at the top of the apparatus and consists of a two layered hodoscope of plastic scintillators paddles (14 paddles per layer). It performs the charge identification of individual nuclear species, providing a measurement of the charge  $Z$  of the incident particle over a wide dynamic range (from  $Z = 1$  up to  $Z = 40$ ).<sup>6</sup> The IMaging Calorimeter (IMC) is a fine grained sampling calorimeter, segmented longitudinally into 16 layers of scintillating fibers (with  $1\text{ mm}^2$  square cross-section), read out individually and arranged in pairs along orthogonal directions. Each pair is interleaved with thin tungsten absorbers (for a total thickness of  $3\text{ X}_0$ ). It reconstructs the early shower profile and the impinging particle trajectory with good angular resolution, while providing also a redundant charge measurement.<sup>1</sup> The third detector is the Total AbSorption Calorimeter (TASC), an homogeneous calorimeter with 12 layers of lead-tungstate (PWO) logs arranged in pairs along orthogonal directions. With its  $27\text{ X}_0$  thickness and shower imaging capability, it measures electrons and gamma-rays with an excellent energy resolution, providing high discrimination against hadronic cascades. The total thickness of the main telescope is equivalent to  $30\text{ X}_0$  and  $1.3$  proton interaction lengths ( $\lambda_I$ ), the geometrical factor is  $0.12\text{ m}^2\text{ sr}$ . A more detailed description of the instrument can be found in Ref. 7 and in the Supplemental Material (SM) of Ref. 9.

## 3. FLIGHT OPERATIONS AND CALIBRATIONS

The commissioning of CALET aboard the ISS was successfully completed at the beginning of October 2015. Since then, the instrument has been taking science data continuously with no significant interruptions.<sup>2</sup> The on-orbit operations are controlled via the JAXA Ground Support Equipment (JAXA-GSE) in Tsukuba by the Waseda CALET Operations Center (WCOC) at Waseda University, Tokyo.

As of April 30, 2021 a total observation time of more than 2027 days was integrated with a live time fraction  $\sim 85\%$  of the total time, and  $\sim 2.7$  billion events collected above 1 GeV. The exposure with the high-energy (HE) trigger mode, designed to maximize the collection power for electrons above 10 GeV, and other high-energy shower events was  $\sim 178\text{ m}^2\text{ sr day}$ .

Energy calibrations of each channel of CHD, IMC, and TASC is performed with penetrating proton and He particles selected in-flight by a dedicated trigger mode. Raw signals are corrected for light output non-uniformity, gain differences among the channels, position and temperature dependence, as well as temporal

gain variations.<sup>7,8</sup> Correlations among the four gain ranges for each TASC channel are calibrated with flight data, and responses from consecutive ranges are linked together to provide a seamless transition. In this way, a dynamic range spanning more than six orders of magnitude is achieved, allowing observations from one minimum ionizing particle to 1 PeV showers.

## 4. COSMIC-RAY DIRECT MEASUREMENTS WITH CALET ON THE ISS

### 4.1. *The Electron Spectrum*

The CALET collaboration reported their first measurement of the inclusive electron+positron spectrum in the energy range from 10 GeV to 3 TeV (Ref. 9) within a fiducial subset of the acceptance. Soon after, the DAMPE Matter Particle Explorer (DAMPE) collaboration published their all-electron spectrum in the energy interval from 25 GeV to 4.6 TeV (Ref. 10).

The latter publication was followed by a number of papers speculating about the origin of a possible peak-like structure near 1.4 TeV in DAMPE data. An updated version of the CALET all-electron spectrum was published, covering the energy

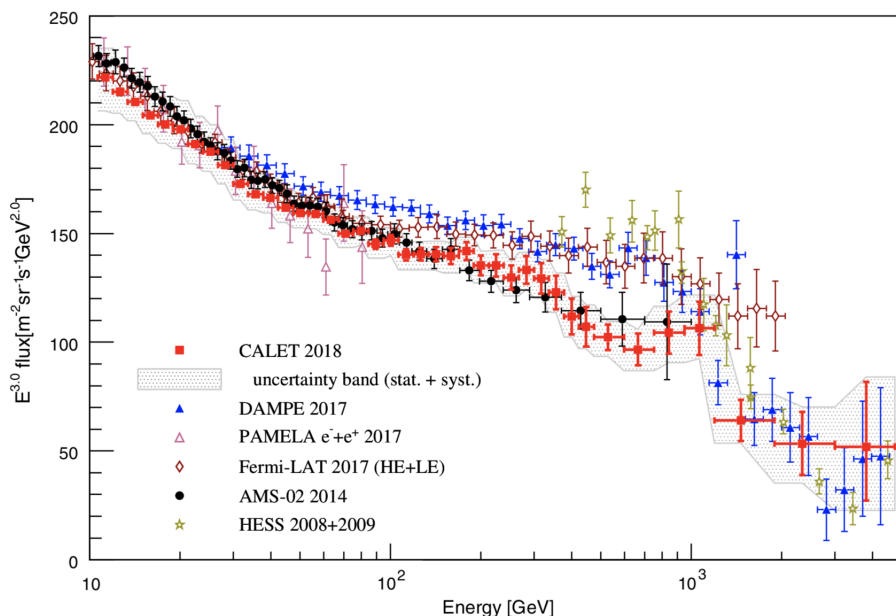


Fig. 1. Direct measurements of the electron + positron flux by space-borne experiments including,<sup>10,11,12–14</sup> and from ground-based experiments.<sup>15,16</sup> The CALET 2018 data<sup>11</sup> are shown as red filled circles in the energy interval 11 GeV to 4.8 TeV. The width of each bin is shown as a horizontal bar, statistical errors as vertical bars. The gray band indicates the quadratic sum of statistical and systematic errors (not including the uncertainty on the energy scale).

range from 11 GeV to 4.8 TeV (Ref. 11) with 780 days of flight data and the full geometrical acceptance. It reported a new analysis with doubled statistics at  $E > 475$  GeV and included one additional energy bin between 3 and 4.8 TeV (Figure 1). The width of each bin is shown as a horizontal bar, the statistical errors as vertical bars, while the gray band is representative of the quadratic sum of statistic and systematic errors. A comprehensive study of the systematic uncertainties was performed as described in Refs. 9, 11 and Supplemental Material therein. A constant electron identification efficiency of 70% was achieved above 30 GeV, with a proton contamination level of 2–5% below 1 TeV and  $\sim 10$ –20% above.

Taking the currently available experimental data at face-value, we notice that the all-electron spectrum data seem to fork into two groups of measurements: AMS-02 + CALET and Fermi/LAT + DAMPE, with good consistency within each group, but with only marginal overlap between the two, possibly indicating the presence of unknown systematic errors. The CALET spectrum is consistent with AMS-02 below  $\sim 1$ TeV where both experiments have a good electron identification capability albeit using different detection techniques. CALET observation of a flux suppression above  $\sim 1$ TeV is consistent with DAMPE within errors. No peak-like structure was found at 1.4 TeV in CALET data, irrespective of the energy binning. After re-binning with the same set of energy bins as DAMPE, an inconsistency between the two measurements emerged<sup>11</sup> with a  $4\sigma$  significance, the latter including the systematic errors quoted by both experiments.

New results on the analysis of electrons based on the first five years of CALET observations will be presented at the upcoming ICRC2021 conference.

#### 4.2. The Proton Spectrum

Cosmic-ray energies from the GeV scale to the multi-TeV region have been explored – in separate subranges – by magnetic spectrometers (e.g., BESS-TeV, PAMELA, and AMS-02), calorimeters (e.g., ATIC, CREAM, NUCLEON, and DAMPE) and Cherenkov / Transition Radiation instruments (e.g., TRACER). In the intermediate energy region from 200 GeV to 800 GeV a deviation from a single power-law (SPL) was observed in both proton and helium spectra by CREAM,<sup>17–19</sup> PAMELA<sup>20,21</sup> and confirmed with high statistics measurements by AMS-02,<sup>22</sup> CALET,<sup>23</sup> and DAMPE.<sup>24</sup>

The first proton paper published by CALET<sup>23</sup> reported a proton flux measurement where, for the first time, a single space-borne instrument was able to cover the whole interval of proton energies from 50 GeV to 10 TeV thanks to its large dynamic range. The proton flux was extracted from the data collected from October 13, 2015 to August 31, 2018 (1054 days) on the ISS using only 40% of the total acceptance. A detailed study of the systematic uncertainties was reported in the same paper and in the Supplementary Material therein.<sup>23</sup> This is of particular relevance because CR flux measurements are well known to be affected by relatively large systematic errors, often specific of each instrument. CALET proton data (Fig. 2)

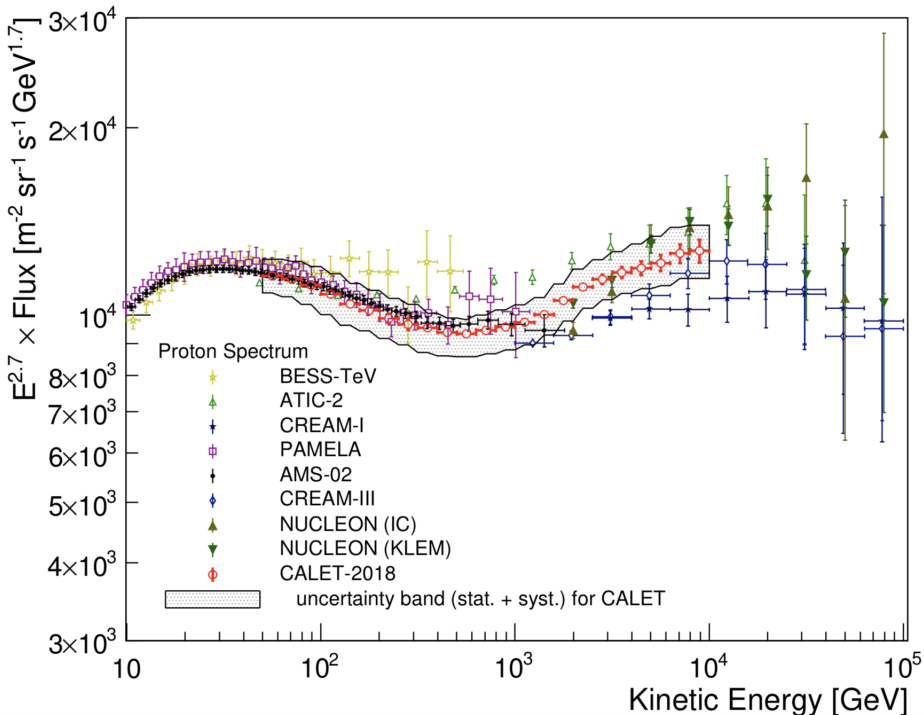


Fig. 2. Cosmic-ray proton spectrum measured by CALET from 50 GeV to 10 TeV published in Ref. 23. The gray band indicates the quadratic sum of statistical and systematic errors.

are consistent with AMS-02 but extend to higher energies by nearly one order of magnitude, showing a very smooth transition of the spectral index from  $-2.81 \pm 0.03$  (in the region 50–500 GeV) to  $-2.56 \pm 0.04$  (in 1–10 TeV), thereby confirming the existence of a spectral hardening and providing evidence of a deviation from a single power law by more than  $3\sigma$ .

An update of CALET proton analysis, based on 5 years of data on the ISS, will be presented at the upcoming ICRC2021 conference together with preliminary results on the helium flux.

#### 4.3. The Spectra of Heavier Nuclei

The observation of a spectral hardening in proton and helium, as well as in carbon and oxygen spectra,<sup>18, 20, 22, 25, 26</sup> have opened a new and unexpected scenario in CR phenomenology. In particular, the high statistics observations by AMS-02, up to a maximum detectable rigidity (MDR) of a few TV, clearly show that primary elements have a very similar rigidity dependence above  $\sim 60$  GV and that secondary elements (like Li, Be and B) also show a flux hardening, though with subtle differences that might be attributed to propagation effects (secondaries propagate first

as primaries and then as secondaries). Therefore, it is very important to extend the presently available measurements to the multi-TeV region and investigate the energy dependence of the spectral index for individual nuclear species with high accuracy. CALET is carrying out extensive measurements of the energy spectra, relative abundances and secondary-to-primary ratios of cosmic-ray nuclei.

Preliminary CALET results on the B/C ratio and on the spectra of heavier nuclei from neon to iron (Fig. 3) were previously reported (see for instance Refs. 4, 27, 28). In the following we will focus on the CALET published spectra of C, O and Fe.

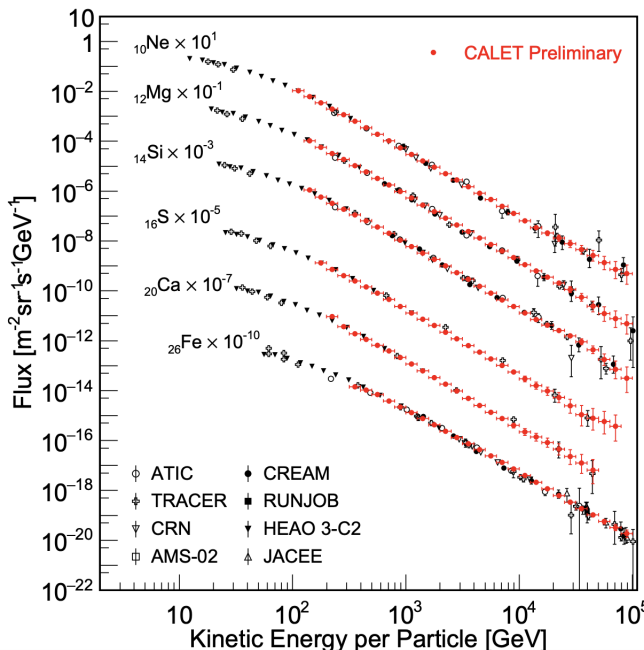


Fig. 3. Preliminary results of energy spectra of heavy primary components of Ne, Mg, Si, S, Ca and Fe as a function of energy per particle compared with previous observations. The Error bars of CALET data<sup>28</sup> represent the statistical uncertainty only.

#### 4.4. Carbon and Oxygen Spectra

The energy spectra of carbon and oxygen and their flux ratio were measured by CALET in the energy range from 10 GeV/n to 2.2 TeV/n and published in Ref. 29. CALET observations (Fig. 4) allow to exclude a single power law spectrum for C and O at the level of more than  $3\sigma$ . A spectral index increase (spectrum flattening)  $\Delta\gamma = 0.166 \pm 0.042$  (carbon) and  $\Delta\gamma = 0.158 \pm 0.053$  (oxygen) were measured above 200 GeV/n, respectively. The fluxes of C and O were found to share the same energy dependence with a constant C/O flux ratio  $0.911 \pm 0.006$  above 25 GeV/n.

While the above results are consistent with the ones reported by AMS-02 for the same elements, the absolute normalization of CALET data is significantly lower than AMS-02, but in agreement with previous experiments (including PAMELA for carbon). For more details please refer to Ref. 29 and the Supplementary Material therein.

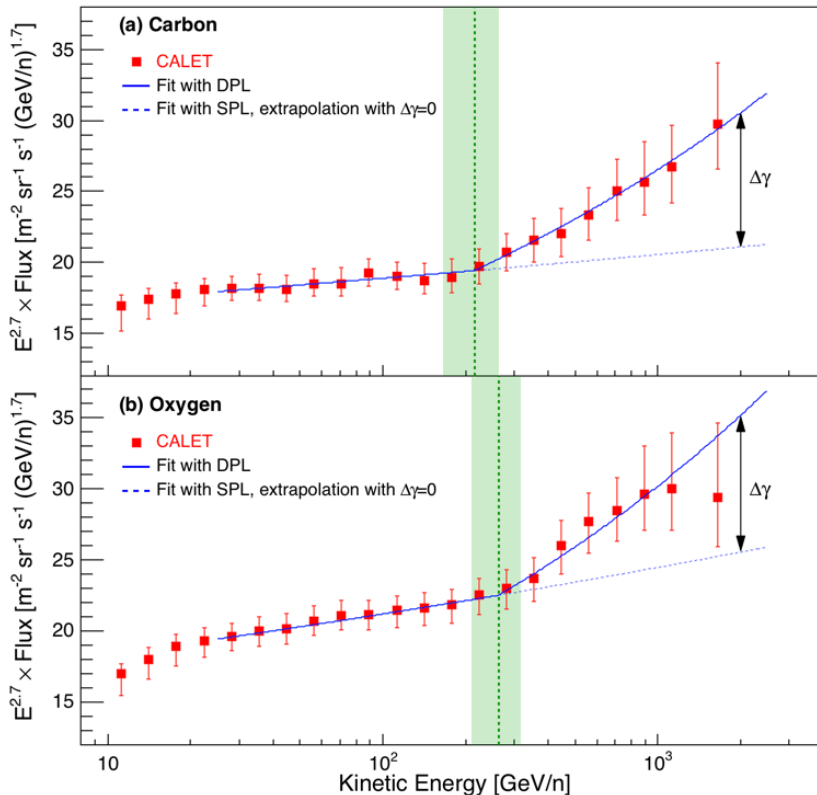


Fig. 4. Fit of the CALET (a) C and (b) O energy spectra<sup>29</sup> with a Double Power Law (DPL) function (blue line) in the energy range [25, 2000]  $\text{GeV}/n$ . The flux is multiplied by  $E^{2.7}$  where  $E$  is the kinetic energy per nucleon. Error bars are the sum in quadrature of statistical and systematic uncertainties. The dashed blue lines represent the extrapolation of an Single Power Law function fitted to the data in the energy range [25, 200]  $\text{GeV}/n$ .  $\Delta\gamma$  is the spectral index change above the transition energy  $E_0$  (vertical green dashed line). The green band shows the uncertainty error on  $E_0$  from the DPL fit.

#### 4.5. The Iron Spectrum

In a recent paper,<sup>30</sup> the CALET collaboration reported their first measurement of the energy spectrum of cosmic-ray iron from 10  $\text{GeV}/n$  to 2.0  $\text{TeV}/n$ .

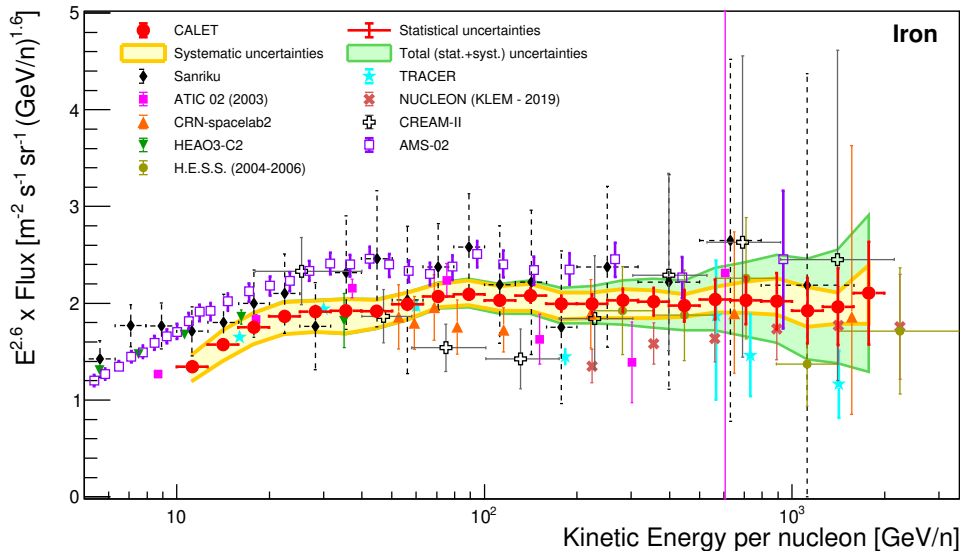


Fig. 5. CALET iron flux<sup>30</sup> as a function of kinetic energy per nucleon in GeV (with multiplicative factor  $E^{2.6}$ ). The error bars of the CALET data (red filled circles) represent the statistical uncertainty only. The yellow band indicates the quadrature sum of systematic errors, while the green band indicates the quadrature sum of statistical and systematic errors. Also plotted are the data points from other direct measurements.<sup>31-39</sup>

The analysis is based on 4.4 years of observations and the measurement achieves a significantly better precision than most of the existing measurements of the same element. The CALET iron differential spectrum in kinetic energy per nucleon is shown in Fig. 5, where uncertainties including statistical and systematic errors are bounded within a green band. The spectrum is compared with the results from space-based (HEAO3-C2,<sup>31</sup> CRN,<sup>32</sup> AMS 02,<sup>33</sup> NUCLEON<sup>34</sup>) and balloon-borne experiments (ATIC-02,<sup>35</sup> TRACER,<sup>36</sup> CREAM-II,<sup>37</sup> Sanriku<sup>38</sup>), as well as ground-based observations (H.E.S.S.<sup>39</sup>). The CALET spectrum is consistent with ATIC 02 and TRACER at low energy and with CRN and HESS at high energy. CALET and NUCLEON iron spectra have similar shapes, while they differ in the absolute normalization of the flux. The latter turns out to be higher for CALET than for CRN by  $\sim 10\%$  on average, while it is lower by  $14\%$  with respect to Sanriku. CALET and AMS-02 iron spectra have a very similar shape (Fig. S12 of the Supplemental Material of Ref. 30), but differ in the absolute normalization of the flux by  $\sim 20\%$ .

Taking into account the average size of the large systematic errors reported in the literature, CALET data turn out to be consistent with previous measurements within the uncertainty error band, both in spectral shape and normalization. Below 50 GeV/n the spectral shape is found to be similar to the one observed for primaries

lighter than iron. Above the same energy, CALET observations are consistent with the hypothesis of an SPL spectrum up to  $2 \text{ TeV}/n$ , i.e., the flattening observed above a few hundred GeV/nucleon in the p-C-O spectra does not appear to be present in the iron spectrum in the sub-TeV region. Beyond this limit, the uncertainties given by the available statistics and large systematics do not allow yet to draw a significant conclusion on a possible deviation from a single power law. An SPL fit in this region yields a spectral index value  $\gamma = -2.60 \pm 0.03$ .

#### 4.6. *The Observation of Gamma-Rays*

CALET can identify gamma-rays and measure their energies from  $\sim 1$  GeV to the TeV region. Both CHD and the first IMC layers are used in the offline analysis as anti-coincidence against incoming charged particles, taking advantage of the high granularity of the IMC.

Gamma-ray candidates are also required to deposit more energy in the bottom IMC layers than in the upper ones where pair conversion takes place. In addition to the HE trigger, CALET implements a LE- $\gamma$  trigger extending the sensitivity to gamma rays with primary energies down to  $\sim 1$  GeV. This dedicated trigger is activated only at low geomagnetic latitudes (to avoid an increase of the dead-time) and it is also enabled whenever a gamma-ray burst is triggered by the Calet Gamma-Ray Burst Monitor (CGBM).<sup>40</sup> The first two years of data allowed a complete characterization of the performance of CALET as a gamma-ray instrument, the optimization of the event selection criteria, the determination of the effective area, Point Spread Function (PSF) and absolute pointing accuracy. Measured signals from gamma-ray bright point sources and diffuse galactic emission were found to be in agreement with simulated results and expectations from Fermi-LAT data.<sup>41</sup> The spectra from sources like Crab, Geminga, and Vela pulsars were measured by CALET and tested for consistency with parameterised LAT spectra. These results confirmed the sensitivity of the calorimeter in observing bright, persistent sources.<sup>42</sup> The gamma-ray sky observed by CALET using the LE- $\gamma$  trigger is shown in Fig. 6.

CALET can also detect gamma-ray transients by means of the CGBM operating in the energy range of 7 keV–20 MeV. As of April 2021, 246 GRBs have been detected, 12% of which were classified as short, with an average rate of  $\sim 44.6$  /year.

A search for electromagnetic counterparts of gravitational waves (GW) triggered by LIGO/Virgo was performed with a combined analysis of the CGBM and the calorimeter. Candidate signals compatible with gamma-ray emission were searched for in time intervals of tens of seconds centered on the reported trigger times of GW151226, GW170104, GW170608, GW170814, and GW170817 events. No signal was detected for all GW events; upper limits on gamma-ray emission were set for GW151226 (CAL + CGBM) and GW170104 (CAL), while GW170608, GW170814, GW170817 turned out to be outside the CALET field-of-view.<sup>43,44</sup>

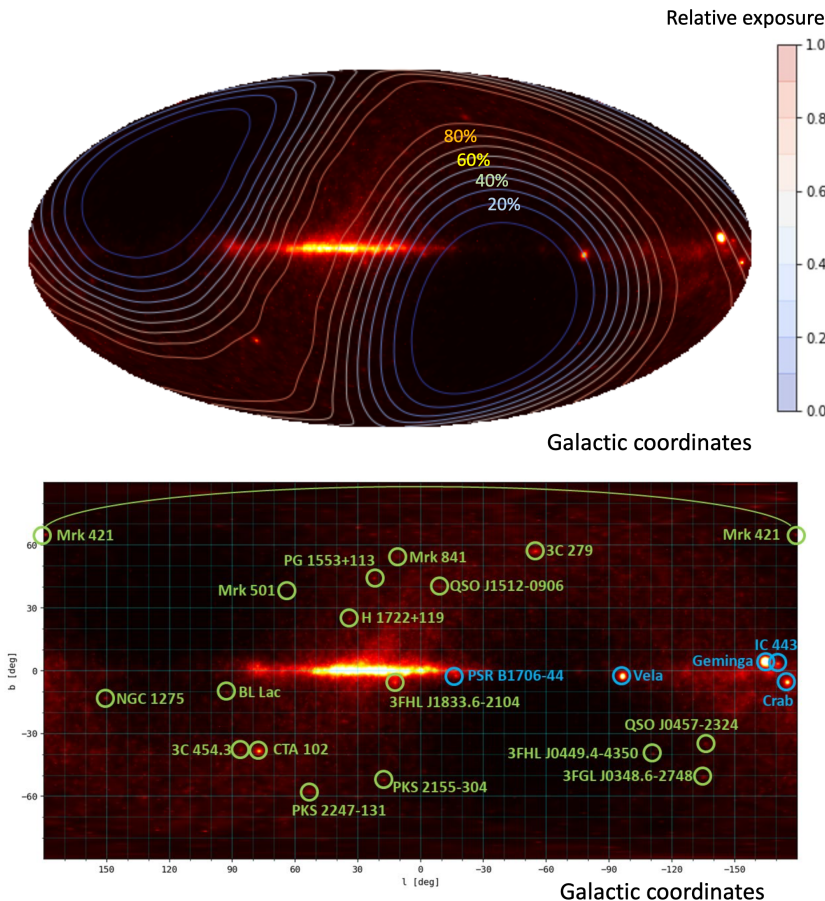


Fig. 6. Top: CALET gamma-ray sky map (observation period: 2015.11.01-2020.07.31) with the LE- $\gamma$  trigger ( $E > 1$  GeV), shown in a Mollweide projection of galactic coordinates. White contours show the relative level of exposure compared to the maximum on the sky; bottom: point sources observed during the same period (with  $> 1$  GeV), including the Crab, Geminga, and Vela pulsars.

## 5. SUMMARY AND PERSPECTIVES

CALET was successfully launched on Aug. 19, 2015. The instrument performance has been very stable during all the scientific observation period from Oct. 13, 2015. CALET measurements of the electron spectrum were published in two papers,<sup>9,11</sup> the latter with improved statistics and extended energy range from 11 GeV to 4.8 TeV. The extension to five years of CALET on-orbit operations provided an increase of the available statistics in the electron observations by a factor  $\sim 3$  thereby contributing to a better understanding of the detector and of the systematic errors. A search for possible spectral footprints of nearby electron sources in the region above  $\sim 1$  TeV is in progress.

The wide dynamic range and excellent charge identification capability allow CALET to measure nuclei in cosmic rays from proton to iron and above, with an energy reach approaching the PeV scale. The proton spectrum was published up to 10 TeV (Ref. 23); C and O spectra to 2.2 TeV/n (Ref. 29), and Fe to 2.0 TeV/n (Ref. 30). The spectral index dependence on energy confirmed a spectral hardening for p, C, O with a smooth onset at a few hundred GeV. Measurements of the energy spectra and composition of all primary and secondary nuclei (and of their ratios) are ongoing. The relative abundance of the ultra heavy nuclei up to  $Z = 40$  has also been preliminarily analyzed.<sup>5</sup>

The performance of the gamma-ray measurements has confirmed CALET's capability to observe the diffuse component and bright point-sources in the gamma-ray sky from  $\sim 1$  GeV to 100 GeV and above (Fig. 6). The continuous GeV gamma-ray sky observation with CALET complements the coverage by other missions and may help to identify unexplored high-energy emissions from future transient events. The latter phenomena are studied with the CGBM.

Follow-up observations were carried out in the X-ray and gamma-ray band of GW events during LIGO/Virgo observation campaigns.<sup>43,44</sup>

Solar modulation is constantly monitored and studied. Since the start of observations in 2015/10, a steady increase in the 1-10 GeV all-electron flux has been observed to present. In the past two years, the flux has reached the maximum flux observed with PAMELA during the previous solar minimum period.<sup>45</sup> Solar energetic particles (SEP) are also studied at high geomagnetic latitudes.

High statistics detection of MeV electrons originating from the radiation belt allows the study of relativistic electron precipitation.<sup>46</sup> This is one of the topics of Space Weather studies<sup>47</sup> which were added as additional observational targets for CALET after the start of on-orbit operations.

Important updates of CALET electron and proton analyses, as well as preliminary results on He, B, B/C analyses, will be presented at the upcoming ICRC2021 conference (highlights in Ref. 48).

The so far excellent performance of the instrument and the outstanding quality of the data suggest that a long-term strategy of CALET observations will contribute to a deeper understanding of cosmic-ray phenomena. CALET operations on the ISS have been recently approved for an extension to the end of 2024 (at least).

## ACKNOWLEDGMENTS

We gratefully acknowledge JAXA's contributions to the development of CALET and to the operations aboard the JEM-EF on the International Space Station. We also wish to express our sincere gratitude to Agenzia Spaziale Italiana (ASI) and NASA for their support of the CALET project. This work was supported in part by JSPS Grant-in-Aid for Scientific Research (S) Number 26220708 and 19H05608, JSPS Grant-in-Aid for Scientific Research (B) Number 17H02901, JSPS Grant-in-Aid for Research Activity Start-up No.20K22352 and by the MEXT-Supported

Program for the Strategic Research Foundation at Private Universities (2011–2015) (No.S1101021) at Waseda University. The CALET effort in Italy is supported by ASI under agreement 2013-018-R.0 and its amendments. The CALET effort in the United States is supported by NASA through Grants No. NNX16AB99G, No. NNX16AC02G, and No. NNH14ZDA001N-APRA-0075.

## References

1. S. Torii (for the CALET Collab.), PoS (ICRC2019) 142 (2019).
2. Y. Asaoka (for the CALET Collab.), PoS (ICRC2019) 001 (2019).
3. S. Torii and P. S. Marrocchesi (for the CALET Collab.), *Adv. Sp. Res.* **64**(12), 2531 (2019).
4. Y. Akaike (for the CALET Collab.), PoS (ICRC2019) 034 (2019).
5. B. F. Rauch (for the CALET Collab.), PoS (ICRC2019) 130 (2019).
6. P. S. Marrocchesi, O. Adriani, Y. Akaike, M. G. Bagliesi, A. Basti, G. Bigongiari, S. Bonechi, M. Bongi, M. Y. Kim, T. Lomtadze, P. Maestro, T. Niita, S. Ozawa, Y. Shimizu, and S. Torii, *Nucl. Instrum. Methods A* **659**, 477 (2011).
7. Y. Asaoka, Y. Akaike, Y. Komiya, R. Miyata, S. Torii, O. Adriani, K. Asano, M. G. Bagliesi, G. Bigongiari, W. R. Binns, S. Bonechi, M. Bongi, P. Brogi, J. H. Buckley, N. Cannady, G. Castellini, et al. (CALET Collab.), *Astropart. Phys.* **91**, 1 (2017).
8. Y. Asaoka, S. Ozawa, S. Torii, O. Adriani, Y. Akaike, K. Asano, M. G. Bagliesi, G. Bigongiari, W. R. Binns, S. Bonechi, M. Bongi, P. Brogi, J. H. Buckley, N. Cannady, G. Castellini, C. Checchia, et al. (CALET Collab.), *Astropart. Phys.* **100**, 29 (2018).
9. O. Adriani, Y. Akaike, K. Asano, Y. Asaoka, M. G. Bagliesi, G. Bigongiari, W. R. Binns, S. Bonechi, M. Bongi, P. Brogi, J. H. Buckley, N. Cannady, G. Castellini, C. Checchia, M. L. Cherry, G. Collazuol, et al. (CALET Collab.), *Phys. Rev. Lett.* **119**, 181101 (2017).
10. G. Ambrosi, Q. An, R. Asfandiyarov, P. Azzarello, P. Bernardini, B. Bertucci, M. S. Cai, J. Chang, D. Y. Chen, H. F. Chen, J. L. Chen, W. Chen, M. Y. Cui, T. S. Cui, A. D'Amone, A. De Benedittis, et al. (DAMPE Collab.), *Nature* **552**, 63 (2017).
11. O. Adriani, Y. Akaike, K. Asano, Y. Asaoka, M. G. Bagliesi, E. Berti, G. Bigongiari, W. R. Binns, S. Bonechi, M. Bongi, P. Brogi, J. H. Buckley, N. Cannady, G. Castellini, C. Checchia, M. L. Cherry, et al. (CALET Collab.), *Phys. Rev. Lett.* **120**, 261102 (2018).
12. O. Adriani, G. C. Barbarino, G. A. Bazilevskaya, R. Bellotti, M. Boezio, E. A. Bogomolov, M. Bongi, V. Bonvicini, S. Bottai, A. Bruno, F. Cafagna, D. Campana, P. Carlson, M. Casolino, G. Castellini, C. De Santis, et al. (PAMELA Collab.), *Riv. Nuovo Cimento* **40**, 473 (2017).
13. S. Abdollahi et al. (The Fermi-LAT Collab.), *Phys. Rev. D* **95**, 082007 (2017).
14. M. Aguilar, D. Aisa, A. Alvino, G. Ambrosi, K. Andeen, L. Arruda, N. Attig, P. Azzarello, A. Bachlechner, F. Barao, A. Barrau, L. Barrin, A. Bartoloni, L. Basara, M. Battarbee, R. Battiston, et al. (AMS Collab.), *Phys. Rev. Lett.* **113**, 221102 (2014).
15. F. Aharonian, A. G. Akhperjanian, U. Barres de Almeida, A. R. Bazer-Bachi, Y. Becherini, B. Behera, W. Benbow, K. Bernlöhr, C. Boisson, A. Bochow, V. Borrel, I. Braun, E. Brion, J. Brucker, P. Brun, R. Bühler, et al. (H.E.S.S. Collab.), *Phys. Rev. Lett.* **101**, 261104, (2008).
16. F. Aharonian, A. G. Akhperjanian, G. Anton, U. Barres de Almeida, A. R. Bazer-Bachi, Y. Becherini, B. Behera, K. Bernlöhr, A. Bochow, C. Boisson, J. Bolmont, V. Borrel, J. Brucker, F. Brun, P. Brun, R. Bühler, et al. (H.E.S.S. Collab.), *Astron. Astrophys.* **508**, 561 (2009).

17. Y. S. Yoon, T. Anderson, A. Barrau, N. B. Conklin, S. Coutu, L. Derome, J. H. Han, J. A. Jeon, K. C. Kim, M. H. Kim, H. Y. Lee, J. Lee, M. H. Lee, S. E. Lee, J. T. Link, A. Menchaca-Rocha, et al., *Astrophys. J.* **839**, 5 (2017).
18. H. S. Ahn, P. Allison, M. G. Bagliesi, J. J. Beatty, G. Bigongiari, J. T. Childers, N. B. Conklin, S. Coutu, M. A. DuVernois, O. Ganel, J. H. Han, J. A. Jeon, K. C. Kim, M. H. Lee, L. Lutz, P. Maestro, et al., *Astrophys. J. Lett.* **714**, L89 (2010).
19. Y. S. Yoon, H. S. Ahn, P. S. Allison, M. G. Bagliesi, J. J. Beatty, G. Bigongiari, P. J. Boyle, J. T. Childers, N. B. Conklin, S. Coutu, M. A. DuVernois, O. Ganel, J. H. Han, J. A. Jeon, K. C. Kim, M. H. Lee, et al., *Astrophys. J.* **728**, 122 (2011).
20. O. Adriani, G. C. Barbarino, G. A. Bazilevskaya, R. Bellotti, M. Boezio, E. A. Bogomolov, L. Bonechi, M. Bongi, V. Bonvicini, S. Borisov, S. Bottai, A. Bruno, F. Cafagna, D. Campana, R. Carbone, P. Carlson, et al. (PAMELA Collab.), *Science* **332**, 69 (2011).
21. O. Adriani, G. C. Barbarino, G. A. Bazilevskaya, R. Bellotti, M. Boezio, E. A. Bogomolov, M. Bongi, V. Bonvicini, S. Borisov, S. Bottai, A. Bruno, F. Cafagna, D. Campana, R. Carbone, P. Carlson, M. Casolino, et al. (PAMELA Collab.), *Astrophys. J.* **765**, 91 (2013).
22. M. Aguilar, D. Aisa, B. Alpat, A. Alvino, G. Ambrosi, K. Andeen, L. Arruda, N. Attig, P. Azzarello, A. Bachlechner, F. Barao, A. Barrau, L. Barrin, A. Bartoloni, L. Basara, M. Battarbee, et al. (AMS Collab.), *Phys. Rev. Lett.* **114**, 171103 (2015).
23. O. Adriani, Y. Akaike, K. Asano, Y. Asaoka, M. G. Bagliesi, E. Berti, G. Bigongiari, W. R. Binns, S. Bonechi, M. Bongi, P. Brogi, A. Bruno, J. H. Buckley, N. Cannady, G. Castellini, C. Checchia, et al. (CALET Collab.), *Phys. Rev. Lett.* **122**, 181102 (2019).
24. Q. An, R. Asfandiyarov, P. Azzarello, P. Bernardini, X. J. Bi, M. S. Cai, J. Chang, D. Y. Chen, H. F. Chen, J. L. Chen, W. Chen, M. Y. Cui, T. S. Cui, H. T. Dai, A. D'Amone, A. De Benedittis, et al. (DAMPE Collab.), *Sci. Adv.* **5** eaax3793 (2019).
25. M. Aguilar, D. Aisa, B. Alpat, A. Alvino, G. Ambrosi, K. Andeen, L. Arruda, N. Attig, P. Azzarello, A. Bachlechner, F. Barao, A. Barrau, L. Barrin, A. Bartoloni, L. Basara, M. Battarbee, et al. (AMS Collab.), *Phys. Rev. Lett.* **115**, 211101 (2015).
26. M. Aguilar, L. Ali Cavasonza, B. Alpat, G. Ambrosi, L. Arruda, N. Attig, S. Aupetit, P. Azzarello, A. Bachlechner, F. Barao, A. Barrau, L. Barrin, A. Bartoloni, L. Basara, S. Başeğmez-du Pree, M. Battarbee, et al. (AMS Collab.), *Phys. Rev. Lett.* **119**, 251101 (2017).
27. P. Maestro, P. S Marrocchesi, G. Bigongiari, and P. Brogi, *Adv. Space Res.* **64**, 2538 (2019).
28. Y. Akaike (for the CALET Collab.), *J. Phys.: Conf. Ser.* **1181**, 012042 (2019).
29. O. Adriani, Y. Akaike, K. Asano, Y. Asaoka, M. G. Bagliesi, E. Berti, G. Bigongiari, W. R. Binns, M. Bongi, P. Brogi, A. Bruno, J. H. Buckley, N. Cannady, G. Castellini, C. Checchia, M. L. Cherry, et al. (CALET Collab.), *Phys. Rev. Lett.* **125**, 251102 (2020).
30. O. Adriani, Y. Akaike, K. Asano, Y. Asaoka, E. Berti, G. Bigongiari, W. R. Binns, M. Bongi, P. Brogi, A. Bruno, J. H. Buckley, N. Cannady, G. Castellini, C. Checchia, M. L. Cherry, G. Collazuol, et al. (CALET Collab.), *Phys. Rev. Lett.* **126**, 241101 (2021).
31. J. J. Engelmann, P. Ferrando, A. Soutoul, P. Goret, E. Juliusson, L. Koch-Miramond, N. Lund, P. Masse, B. Peters, N. Petrou, and I. L. Rasmussen, *Astron. Astrophys.* **233**, 96 (1990).
32. D. Müller, S. P. Swordy, P. Meyer, J. L'Heureux, and J. M. Grunsfeld, *Astrophys. J.* **374**, 356 (1991).
33. M. Aguilar, L. Ali Cavasonza, M. S. Allen, B. Alpat, G. Ambrosi, L. Arruda, N. Attig, F. Barao, L. Barrin, A. Bartoloni, S. Başeğmez-du Pree, R. Battiston, M. Behlmann,

B. Beischer, J. Berdugo, B. Bertucci, et al. (AMS Collab.), *Phys. Rev. Lett.* **126**, 041104 (2021).

34. V. Grebenyuk, D. Karmanov, I. Kovalev, I. Kudryashov, A. Kurganov, A. Panov, D. Podorozhny, A. Tkachenko, L. Tkachev, A. Turundaevskiy, O. Vasiliev, A. Voronin (NUCLEON Collaboration), *Adv. Space Res.* **64**, 2546 (2019).
35. A. D. Panov, J. H. Adams, H. S. Ahn, G. L. Bashinzhagyan, J. W. Watts, J. P. Wefel, J. Wu, O. Ganel, T. G. Guzik, V. I. Zatsepin, I. Isbert, K. C. Kim, M. Christl, E. N. Kouznetsov, M. I. Panasyuk, E. S. Seo, et al. (ATIC Collaboration), *Bull. Russ. Acad. Sci.* **73**, 564 (2009).
36. M. Ave, P. J. Boyle, F. Gahbauer, C. Höppner, J. R. Hörandel, M. Ichimura, D. Müller, and A. Romero-Wolf (TRACER Collab.), *Astrophys. J.* **678**, 262 (2008).
37. H. S. Ahn, P. Allison, M. G. Bagliesi, L. Barbier, J. J. Beatty, G. Bigongiari, T. J. Brandt, J. T. Childers, N. B. Conklin, S. Coutu, M. A. DuVernois, O. Ganel, J. H. Han, J. A. Jeon, K. C. Kim, M. H. Lee, et al. (CREAM Collab.), *Astrophys. J.* **707**, 593 (2009).
38. M. Ichimura, M. Kogawa, S. Kuramata, H. Mito, T. Murabayashi, H. Nanjo, T. Nakamura, K. Ohba, T. Ohuchi, T. Ozawa, Y. Yamada, H. Matsutani, Z. Watanabe, E. Kamioka, K. Kirii, M. Kitazawa, et al., *Phys. Rev. D* **48**, 1949 (1993).
39. F. Aharonian, A. G. Akhperjanian, A. R. Bazer-Bachi, M. Beilicke, W. Benbow, D. Berge, K. Bernlöhr, C. Boisson, O. Bolz, V. Borrel, I. Braun, E. Brion, A. M. Brown, R. Bühler, I. Büsching, S. Carrigan, et al. (H.E.S.S. Collab.), *Phys. Rev. D* **75**, 042004 (2007).
40. K. Yamaoka, A. Yoshida, T. Sakamoto, I. Takahashi, T. Hara, T. Yamamoto, Y. Kawakubo, R. Inoue, S. Terazawa, R. Fujioka, K. Senuma, S. Nakahira, H. Tomida, S. Ueno, S. Torii, M. L. Cherry, S. Ricciarini (CALET Collab.), in *Proceedings of the 7th Huntsville Gamma-Ray Burst Symposium, GRB 2013, eConf C1304143*, 41 (2013).
41. N. Cannady, Y. Asaoka, F. Satoh, M. Tanaka, S. Torii, M. L. Cherry, M. Mori, O. Adriani, Y. Akaike, K. Asano, M. G. Bagliesi, E. Berti, G. Bigongiari, W. R. Binns, S. Bonechi, M. Bongi, et al. (CALET Collab.), *Astrophys. J. Suppl. S.* **238**, 5 (2018).
42. M. Mori et al. (for the CALET Collab.), PoS (ICRC2019) 586 (2019).
43. O. Adriani, Y. Akaike, K. Asano, Y. Asaoka, M. G. Bagliesi, E. Berti, G. Bigongiari, W. R. Binns, S. Bonechi, M. Bongi, P. Brogi, J. H. Buckley, N. Cannady, G. Castellini, C. Checchia, M. L. Cherry, et al. (CALET Collab.), *Astrophys. J. Lett.* **863**, 160 (2018).
44. O. Adriani, Y. Akaike, K. Asano, Y. Asaoka, M. G. Bagliesi, G. Bigongiari, W. R. Binns, S. Bonechi, M. Bongi, P. Brogi, J. H. Buckley, N. Cannady, G. Castellini, C. Checchia, M. L. Cherry, G. Collazuol, et al. (CALET Collab.), *Astrophys. J. Lett.* **829**, L20 (2016).
45. S. Miyake et al. (for the CALET Collab.), PoS (ICRC2019) 1126 (2019).
46. R. Kataoka, Y. Asaoka, S. Torii, T. Terasawa, S. Ozawa, T. Tamura, Y. Shimizu, Y. Akaike, M. Mori (CALET Collab.), *Geophys. Res. Lett.* **43**, 4119 (2016).
47. A. Bruno et al. (for the CALET Collab.), PoS (ICRC2019) 1063 (2019).
48. P. S. Marrocchesi et al. (for the CALET Collab.), PoS (ICRC2021) 010 (2021).

## Full Authors List: CALET Collaboration

O. Adriani<sup>1,2</sup>, Y. Akaike<sup>3,4</sup>, K. Asano<sup>5</sup>, Y. Asaoka<sup>5</sup>, E. Berti<sup>1,2</sup>, G. Bigongiari<sup>6,7</sup>, W. R. Binns<sup>8</sup>, M. Bongi<sup>1,2</sup>, P. Brogi<sup>6,7</sup>, A. Bruno<sup>9,10</sup>, J. H. Buckley<sup>8</sup>, N. Cannady<sup>11,12,13</sup>, G. Castellini<sup>14</sup>, C. Checchia<sup>6</sup>, M. L. Cherry<sup>15</sup>, G. Collazuol<sup>16,17</sup>, K. Ebisawa<sup>18</sup>, A. W. Ficklin<sup>15</sup>, H. Fukue<sup>18</sup>, S. Gonzi<sup>1,2</sup>, T. G. Guzik<sup>15</sup>, T. Hams<sup>11</sup>, K. Hibino<sup>19</sup>, M. Ichimura<sup>20</sup>, K. Ioka<sup>21</sup>, W. Ishizaki<sup>5</sup>, M. H. Israel<sup>8</sup>, K. Kasahara<sup>22</sup>, J. Kataoka<sup>23</sup>, R. Kataoka<sup>24</sup>, Y. Katayose<sup>25</sup>, C. Kato<sup>26</sup>, N. Kawanaka<sup>27,28</sup>, Y. Kawakubo<sup>15</sup>, K. Kobayashi<sup>3,4</sup>, K. Kohri<sup>29</sup>, H. S. Krawczynski<sup>8</sup>, J. F. Krizmanic<sup>11,12,13</sup>, P. Maestro<sup>6,7</sup>, P. S. Marrocchesi<sup>6,7</sup>, A. M. Messineo<sup>30,7</sup>, J. W. Mitchell<sup>12</sup>, S. Miyake<sup>32</sup>, A. A. Moiseev<sup>33,12,13</sup>, M. Mori<sup>34</sup>, N. Mori<sup>2</sup>, H. M. Motz<sup>35</sup>, K. Munakata<sup>26</sup>, S. Nakahira<sup>18</sup>, J. Nishimura<sup>18</sup>, G. A. de Nolfo<sup>9</sup>, S. Okuno<sup>19</sup>, J. F. Ormes<sup>36</sup>, N. Ospina<sup>16,17</sup>, S. Ozawa<sup>37</sup>, L. Pacini<sup>1,14,2</sup>, P. Papini<sup>2</sup>, B. F. Rauch<sup>8</sup>, S. B. Ricciarini<sup>14,2</sup>, K. Sakai<sup>11,12,13</sup>, T. Sakamoto<sup>38</sup>, M. Sasaki<sup>33,12,13</sup>, Y. Shimizu<sup>19</sup>, A. Shiomii<sup>39</sup>, P. Spillantini<sup>1</sup>, F. Stolzi<sup>6,7</sup>, S. Sugita<sup>38</sup>, A. Sulaj<sup>6,7</sup>, M. Takita<sup>5</sup>, T. Tamura<sup>19</sup>, T. Terasawa<sup>40</sup>, S. Torii<sup>3</sup>, Y. Tsunesada<sup>41</sup>, Y. Uchihori<sup>42</sup>, E. Vannuccini<sup>2</sup>, J. P. Wefel<sup>15</sup>, K. Yamaoka<sup>43</sup>, S. Yanagita<sup>44</sup>, A. Yoshida<sup>38</sup>, K. Yoshida<sup>22</sup>, and W. V. Zober<sup>8</sup>

<sup>1</sup>Department of Physics, University of Florence, Via Sansone, 1, 50019 Sesto, Fiorentino, Italy, <sup>2</sup>INFN Sezione di Florence, Via Sansone, 1, 50019 Sesto, Fiorentino, Italy, <sup>3</sup>Waseda Research Institute for Science and Engineering, Waseda University, 17 Kikuicho, Shinjuku, Tokyo 162-0044, Japan, <sup>4</sup>JEM Utilization Center, Human Spaceflight Technology Directorate, Japan Aerospace Exploration Agency, 2-1-1 Sengen, Tsukuba, Ibaraki 305-8505, Japan, <sup>5</sup>Institute for Cosmic Ray Research, The University of Tokyo, 5-1-5 Kashiwa-no-Ha, Kashiwa, Chiba 277-8582, Japan, <sup>6</sup>Department of Physical Sciences, Earth and Environment, University of Siena, via Roma 56, 53100 Siena, Italy, <sup>7</sup>INFN Sezione di Pisa, Polo Fibonacci, Largo B. Pontecorvo, 3, 56127 Pisa, Italy, <sup>8</sup>Department of Physics and McDonnell Center for the Space Sciences, Washington University, One Brookings Drive, St. Louis, Missouri 63130-4899, USA, <sup>9</sup>Heliospheric Physics Laboratory, NASA/GSFC, Greenbelt, Maryland 20771, USA, <sup>10</sup>Department of Physics, Catholic University of America, Washington, DC 20064, USA, <sup>11</sup>Center for Space Sciences and Technology, University of Maryland, Baltimore County, 1000 Hilltop Circle, Baltimore, Maryland 21250, USA, <sup>12</sup>Astroparticle Physics Laboratory, NASA/GSFC, Greenbelt, Maryland 20771, USA, <sup>13</sup>Center for Research and Exploration in Space Sciences and Technology, NASA/GSFC, Greenbelt, Maryland 20771, USA, <sup>14</sup>Institute of Applied Physics (IFAC), National Research Council (CNR), Via Madonna del Piano, 10, 50019 Sesto, Fiorentino, Italy, <sup>15</sup>Department of Physics and Astronomy, Louisiana State University, 202 Nicholson Hall, Baton Rouge, Louisiana 70803, USA, <sup>16</sup>Department of Physics and Astronomy, University of Padova, Via Marzolo, 8, 35131 Padova, Italy, <sup>17</sup>INFN Sezione di Padova, Via Marzolo, 8, 35131 Padova, Italy, <sup>18</sup>Institute of Space and Astronautical Science, Japan Aerospace Exploration Agency, 3-1-1 Yoshinodai, Chuo, Sagamihara, Kanagawa 252-5210, Japan, <sup>19</sup>Kanagawa University, 3-27-1 Rokkakubashi, Kanagawa, Yokohama, Kanagawa 221-8686, Japan, <sup>20</sup>Faculty of Science and Technology, Graduate School of Science and Technology, Hirosaki University, 3, Bunkyo, Hirosaki, Aomori 036-8561, Japan, <sup>21</sup>Yukawa Institute for Theoretical Physics, Kyoto University, Kitashirakawa Oiwakecho, Sakyo, Kyoto 606-8502, Japan, <sup>22</sup>Department of Electronic Information Systems, Shibaura Institute of Technology, 307 Fukasaku, Minuma, Saitama 337-8570, Japan, <sup>23</sup>School of Advanced Science and Engineering, Waseda University, 3-4-1 Okubo, Shinjuku, Tokyo 169-8555, Japan, <sup>24</sup>National Institute of Polar Research, 10-3, Midori-cho, Tachikawa, Tokyo 190-8518, Japan, <sup>25</sup>Faculty of Engineering, Division of Intelligent Systems Engineering, Yokohama National University, 79-5 Tokiwadai, Hodogaya, Yokohama 240-8501, Japan, <sup>26</sup>Faculty of Science, Shinshu University, 3-1-1 Asahi, Matsumoto, Nagano 390-8621, Japan, <sup>27</sup>Hakubi Center, Kyoto University, Yoshida Honmachi, Sakyo-ku, Kyoto 606-8501, Japan, <sup>28</sup>Department of Astronomy, Graduate School of Science, Kyoto University, Kitashirakawa Oiwake-cho, Sakyo-ku, Kyoto 606-8502, Japan, <sup>29</sup>Institute of Particle and Nuclear Studies, High Energy Accelerator Research Organization, 1-1 Oho, Tsukuba, Ibaraki 305-0801, Japan, <sup>30</sup>University of Pisa, Polo Fibonacci, Largo B. Pontecorvo, 3, 56127 Pisa, Italy, <sup>31</sup>Astroparticle Physics Laboratory, NASA/GSFC, Greenbelt, Maryland 20771, USA, <sup>32</sup>Department of Electrical and Electronic Systems Engineering, National Institute of Technology, Ibaraki College, 866 Nakane, Hitachinaka, Ibaraki 312-8508, Japan, <sup>33</sup>Department of Astronomy, University of Maryland, College Park, Maryland 20742, USA, <sup>34</sup>Department of Physical Sciences, College of Science and Engineering, Ritsumeikan University, Shiga 525-8577, Japan, <sup>35</sup>Faculty of Science and Engineering, Global Center for Science and Engineering, Waseda University, 3-4-1 Okubo, Shinjuku, Tokyo 169-8555, Japan, <sup>36</sup>Department of Physics and Astronomy, University of Denver, Physics Building, Room 211, 2112 East Wesley Avenue, Denver, Colorado 80208-6900, USA, <sup>37</sup>Quantum ICT Advanced Development Center, National Institute of Information and Communications Technology, 4-2-1 Nukui-Kitamachi, Koganei, Tokyo 184-8795, Japan, <sup>38</sup>College of Science and Engineering, Department of Physics and Mathematics, Aoyama Gakuin University, 5-10-1 Fuchinobe, Chuo, Sagamihara, Kanagawa 252-5258, Japan, <sup>39</sup>College of Industrial Technology, Nihon University, 1-2-1 Izumi, Narashino, Chiba 275-8575, Japan, <sup>40</sup>RIKEN, 2-1 Hirosawa, Wako, Saitama 351-0198, Japan, <sup>41</sup>Division of Mathematics and Physics, Graduate School of Science, Osaka City University, 3-3-138 Sugimoto, Sumiyoshi, Osaka 558-8585, Japan, <sup>42</sup>National Institutes for Quantum and Radiation Science and Technology, 4-9-1 Anagawa, Inage, Chiba 263-8555, Japan, <sup>43</sup>Nagoya University, Furo, Chikusa, Nagoya 464-8601, Japan, <sup>44</sup>College of Science, Ibaraki University, 2-1-1 Bunkyo, Mito, Ibaraki 310-8512, Japan